Improving the parameterization of dust emission threshold in the Community Earth System Model (CESM)

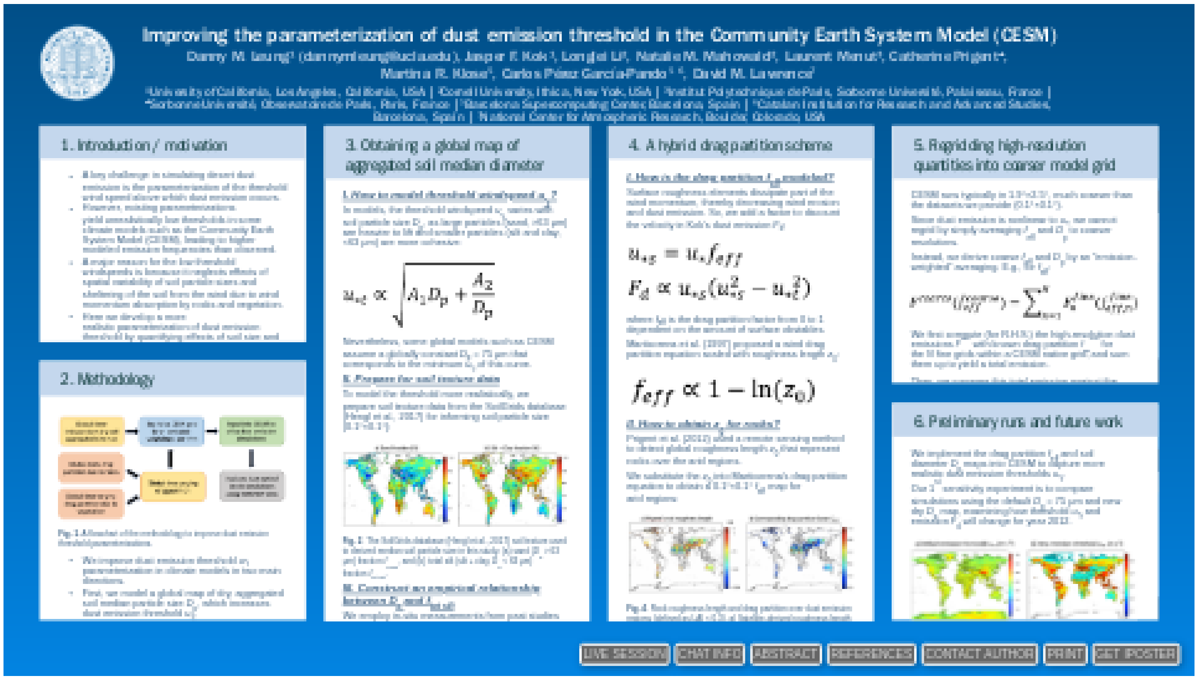

Danny M. Leung[1] (dannymleung@ucla.edu), Jasper F. Kok[1], Longlei Li[2], Natalie M. Mahowald[2], Laurent Menut[3], Catherine Prigent[4], Martina R. Klose[5], Carlos Pérez García-Pando[5 6], David M. Lawrence[7]

[1]University of California, Los Angeles, California, USA | [2]Cornell University, Ithica, New York, USA | [3]Institut Polytechnique de Paris, Sorbonne Université, Palaiseau, France | [4]Sorbonne Université, Observatoire de Paris, Paris, France | [5]Barcelona Supercomputing Center, Barcelona, Spain | [6]Catalan Institution for Research and Advanced Studies, Barcelona, Spain | [7]National Center for Atmospheric Research, Boulder, Colorado, USA

PRESENTED AT:

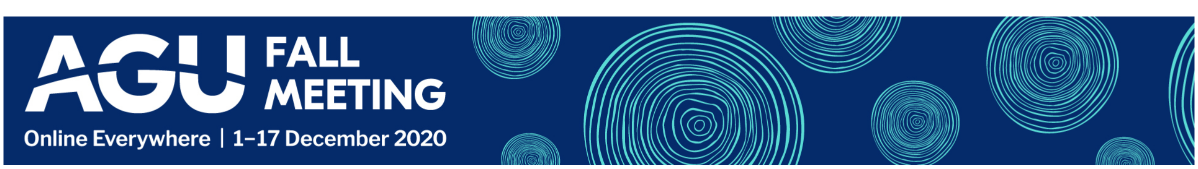

1. INTRODUCTION / MOTIVATION

- A key challenge in simulating desert dust emission is the parameterization of the threshold wind speed above which dust emission occurs.
- However, existing parameterizations yield unrealistically low thresholds in some climate models such as the Community Earth System Model (CESM), leading to higher modeled emission frequencies than observed.
- A major reason for the low threshold windspeeds is because it neglects effects of spatial variability of soil particle sizes and sheltering of the soil from the wind due to wind momentum absorption by rocks and vegetation.
- Here we develop a more realistic parameterization of dust emission threshold by **quantifying effects of soil size and wind drag partition**.

2. METHODOLOGY

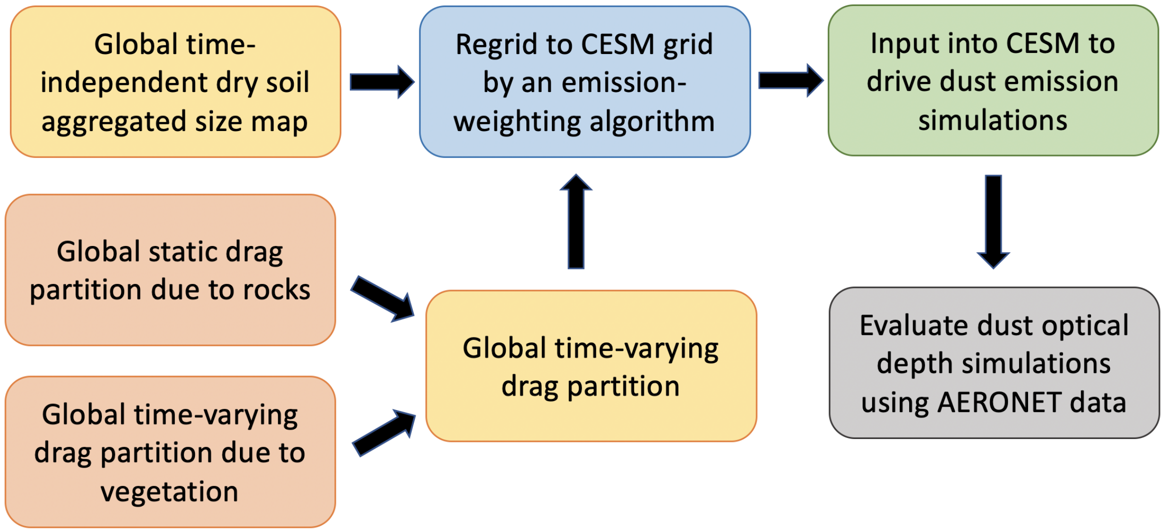

Fig. 1. A flowchart of the methodology to improve dust emission threshold parameterizations.

- We improve dust emission threshold u_{*t} parameterization in climate models in two main directions.
- First, we model a global map of dry, aggregated soil median particle size D_p, which increases dust emission threshold u_{*t}.
- Second, we account for dissipations of surface wind due to roughness elements including rocks and vegetation using a drag partition factor f_{eff}, which decreases wind frictional velocity u_*.
- We then use an "emission-weighted" averaging algorithm to regrid high-resolution (0.1°) datasets to CESM grid (1.9°×2.5°) or any other model native grids.
- We implement the regridded datasets into the CESM and examine the corresponding changes in modeled dust emissions and aerosol optical depth (AOD).

In this study, we use the Kok et al. (2014b) dust emission equation combined with the Shao and Lu (2000) dust emission threshold equation. Kok et al. (2014b) equation calculates dust flux in kg m^{-2} s^{-1}:

$$F_d \propto u_*(u_*^2 - u_{*t}^2)$$

$$u_* > u_{*t}$$

We will implement the modifications in this paper to another default emission scheme (Zender et al., 2003) in CESM in future.

3. OBTAINING A GLOBAL MAP OF AGGREGATED SOIL MEDIAN DIAMETER

I. How to model threshold windspeed u_{*t}?

In models, the threshold windspeed u_{*t} varies with soil particle size D_p, as large particles (sand, >63 μm) are heavier to lift and smaller particles (silt and clay, <63 μm) are more cohesive:

$$u_{*t} \propto \sqrt{A_1 D_p + \frac{A_2}{D_p}}$$

Nevertheless, some global models such as CESM assume a globally constant D_p = 75 μm that corresponds to the minimum u_{*t} of this curve.

II. Prepare for soil texture data

To model the threshold more realistically, we prepare soil texture data from the SoilGrids database (Hengl et al., 2017) for informing soil particle size (0.1°×0.1°):

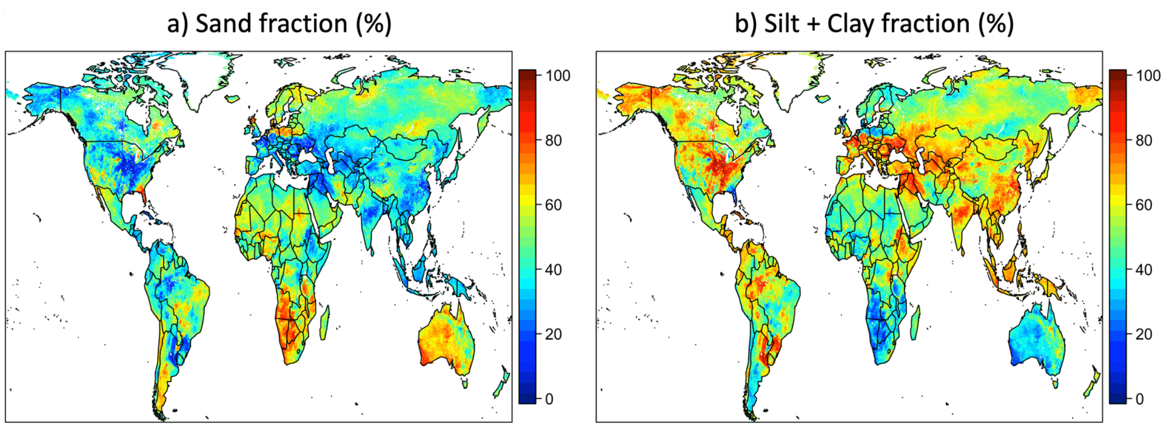

Fig. 2. The SoilGrids database (Hengl et al., 2017) soil texture used to derived median soil particle size in this study. (a) sand (D_p > 63 μm) fraction f_{sand}, and (b) total silt (silt + clay, D_p < 63 μm) fraction $f_{tot\ silt}$.

III. Construct an empirical relationship between D_p and $f_{tot\ silt}$

We employ in-situ measurements from past studies and found strong relationships between the dry soil aggregate D_p and the total silt fraction $f_{tot\ silt} = f_{clay} + f_{silt}$.

$f_{tot\ silt}$ is likely a good indicator for soil particle cohesion since silt and clay are "glue" in soil.

Although the relationship is much weaker for desert soils, they in general have larger D_p than CESM assumed.

Projecting the linear relations on the SoilGrids soil textures yield a new global D_p map. Here we define MODIS leaf area index (LAI) < 0.3 as arid regions and otherwise as non-arid regions.

We yield much larger soil D_p than 75 μm around the globe over both arid and non-arid regions.

We will input this map into CESM to calculate a new map of dust emission threshold u_{*t} (see Fig. 7), expecting u_{*t} to increase.

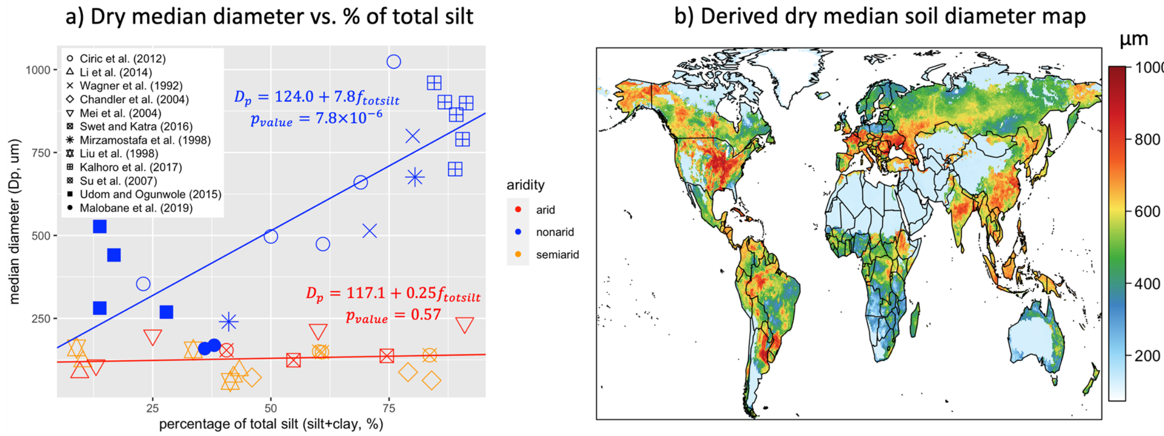

Fig. 3. The global soil diameter map (in µm) derived from the Soilgrids (Hengl et al., 2017) soil texture data. (a) A scatterplot of soil particle diameter vs. % of total silt $f_{\text{tot silt}}$. (b) A global median dry soil diameter map derived using the relation in Fig. 3a and soil texture ($f_{\text{tot silt}}$) from Fig. 2.

We will explore other possible predictors such as soil organic carbon (SOC), pH, and $CaCO_3$ to explain and predict D_p in the future.

Note: it is important to characterize the soil particle "aggregated" size obtained by "dry" sieving in laboratories, since wet sieving will wash and disaggregate soil particles that adhere together (Chatenet et al., 1996). We only use soil studies that employed dry sieving here.

4. A HYBRID DRAG PARTITION SCHEME

I. How is the drag partition f_{eff} modeled?

Surface roughness elements dissipate part of the wind momentum, thereby decreasing wind erosion and dust emission. So, we add a factor to discount the velocity in Kok's dust emission F_d:

$$u_{*s} = u_* f_{eff}$$

$$F_d \propto u_{*s}(u_{*s}^2 - u_{*t}^2)$$

where f_{eff} is the drag partition factor from 0 to 1 dependent on the amount of surface obstables.

Marticorena et al. (1997) proposed a wind drag partition equation scaled with **roughness length z_0**, which characterizes the amount of obstacles:

$$f_{eff} \propto 1 - \ln(z_0)$$

II. How to obtain z_0 for rocks?

Prigent et al. (2012) used a remote sensing method to detect global roughness length z_0 that represent rocks over the arid regions.

We substitute the z_0 into Marticorena's drag partition equation to obtain a 0.1°×0.1° f_{eff} map for arid regions:

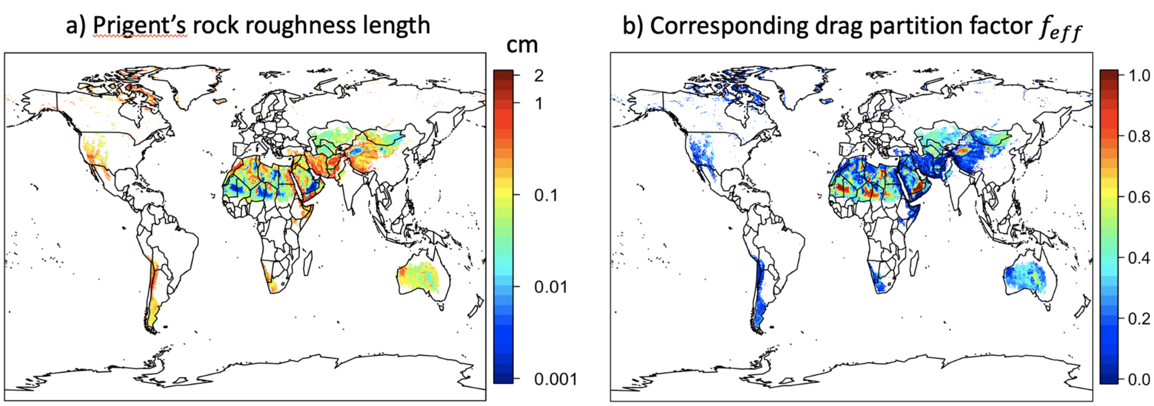

Fig. 4. Rock roughness length and drag partition over dust emission regions (defined as LAI < 0.3). a) Satellite-derived roughness length (z_0) obtained by Prigent et al. (2012). b) The corresponding drag partition factor (f_{eff}) by substituting z_0 into Marticorena's 1997 drag partition equation.

III. How to obtain z_0 for vegetation?

For vegetation, we implement a parameterization for time-varying roughness of vegetation using MODIS leaf area index (LAI) (Pierre et al., 2012; Klose et al., submitted). In Klose's model, z_0 is a function of LAI:

$$z_0 \propto \mathrm{LAI}^3$$

And this roughness length is substituted back to Marticorena's equation for yielding the f_{eff} map for vegetation.

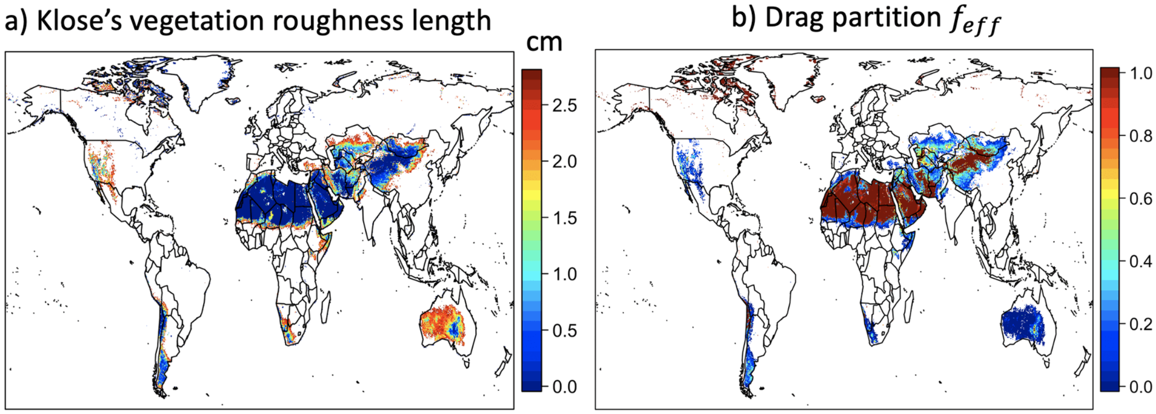

Fig. 5. Klose's parameterization of (a) vegetation roughness length z_0, and the corresponding (b) drag partition f_{eff}.

IV. How to combine the drag partition effects from both rocks and vegetation?

For any timestep, when the vegetation roughness is larger than the rock roughness, we will use vegetation roughness instead for computing drag partition in climate models (plants grow and rocks do not!).

5. REGRIDDING HIGH-RESOLUTION QUANTITIES INTO COARSER MODEL GRID

CESM runs typically in 1.9°×2.5°, much coarser than the datasets we provide (0.1°×0.1°).

Since dust emission is nonlinear to u_*, we cannot regrid by simply averaging f_{eff} and D_{p} to coarser resolutions.

Instead, we derive coarse f_{eff} and D_{p} by an "emission-weighted" averaging. E.g., for f_{eff}:

$$F^{coarse}(\hat{f}_{eff}^{coarse}) = \sum_{n=1}^{N} F_n^{fine}(f_{eff,n}^{fine})$$

We first compute (for R.H.S.) the high-resolution dust emissions F^{fine} with known drag partition f_{eff}^{fine} for the N fine grids within a CESM native grid, and sum them up to yield a total emission.

Then, we compare this total emission against the CESM-modeled emission F^{coarse} (L.H.S.) to estimate the required coarse $f_{\mathrm{eff}}^{\mathrm{coarse}}$ for CESM (Fig. 6).

This emission-weighted approach will always generate a higher f_{eff} than aspatially averaged f_{eff}, except when f_{eff} is already close to 1 (Fig. 6d).

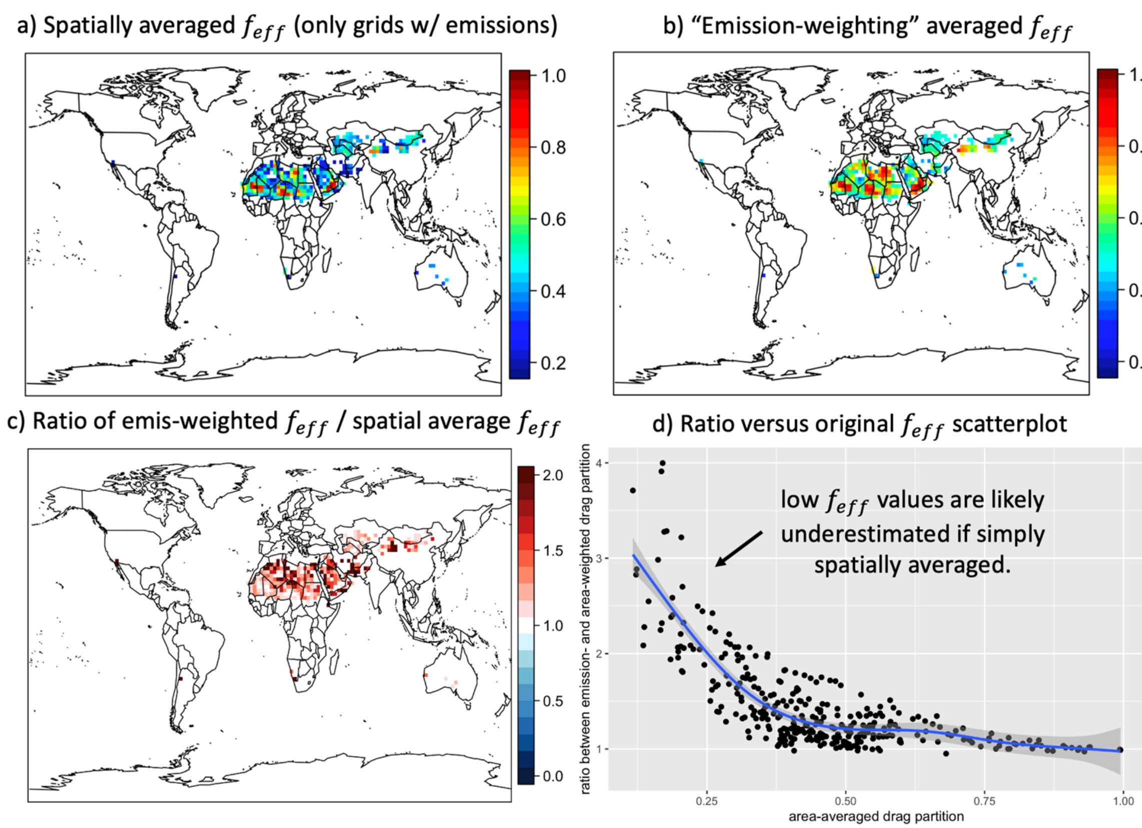

Fig. 6. The difference between using a simple spatial averaging and "emission-weighted averaging" approach to yield drag partition factor f_{eff} in CESM (coarse) resolution. (a) a spatial average of high-resolution f_{eff} (Fig. 4b) to CESM grid. (b) The "emission-weighted" average drag partition factor f_{eff} in CESM resolution. (c) Ratio of emission-weighted f_{eff} (Fig. 6b) and to spatially averaged f_{eff} (Fig. 6a). (d) The ratio in Fig. 6c. vs. the spatially averaged f_{eff} in Fig. 6b.

Note: our method is general and can generate D_{p} and f_{eff} data at any resolution, for any other atmospheric and climate models (coarser than 0.1°×0.1°). We will make the data available for other models to use.

6. PRELIMINARY RUNS AND FUTURE WORK

We implement the drag partition f_{eff} and soil diameter D_p maps into CESM to capture more realistic dust emission thresholds u_{*t}.

Our 1st sensitivity experiment is to compare simulations using the default D_p = 75 µm and new dry D_p map, examining how threshold u_{*t} and emission F_d will change for year 2012.

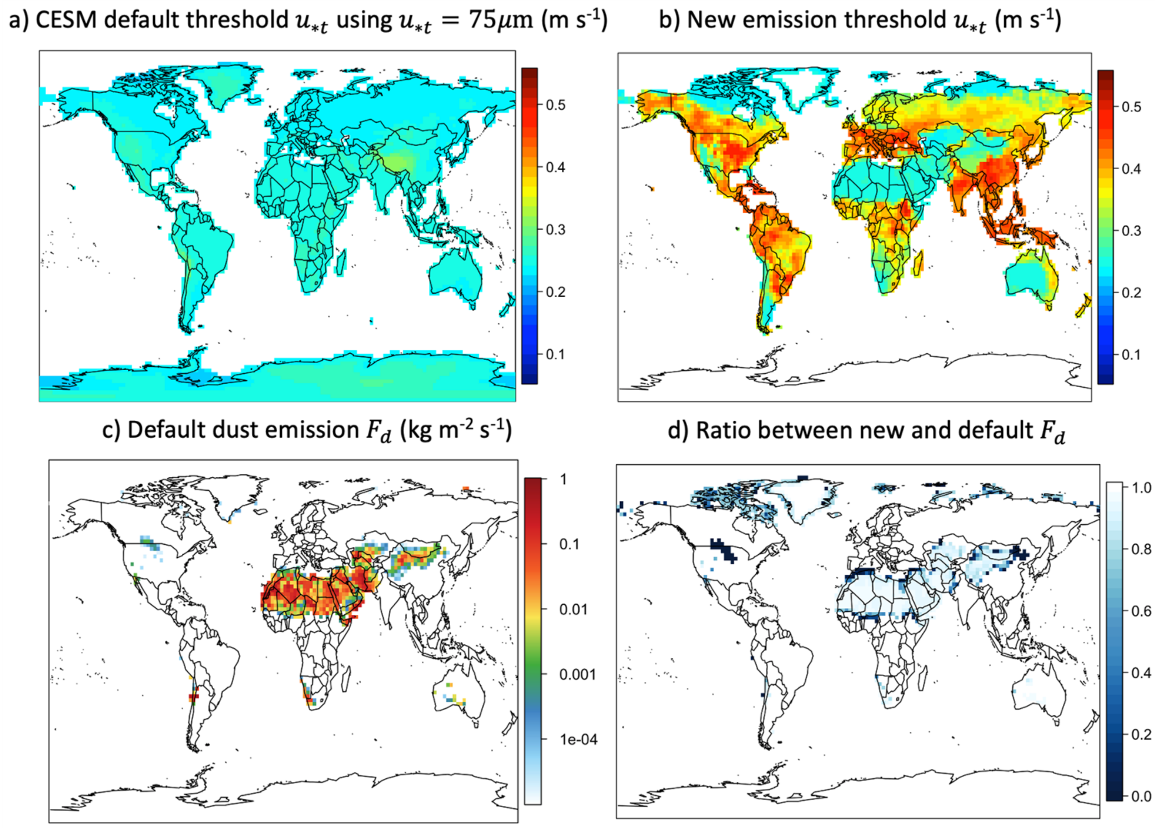

Fig. 7. A CESM sensitivity experiment to copmare simulations using the default D_p = 75 µm and new dry D_p map, for 2012. (a, b) The dust emission threshold u_{*t} simulated using (a) globally constant D_p = 75 µm and (b) global soil size (Fig. 3). (c) The simulated default total dust emissions F_d (kg / m2 / yr) with globally constant D_p as calculated by Kok et al. (2014). (d) The ratio between the new emissions with globally varying D_p map and the default emissions with globally constnt D_p.

Our 2nd sensitivity experiment is to compare runs with and without the static drag partition effect f_{eff} for rocks, examining how threshold dust emission F_d will change for year 2012.

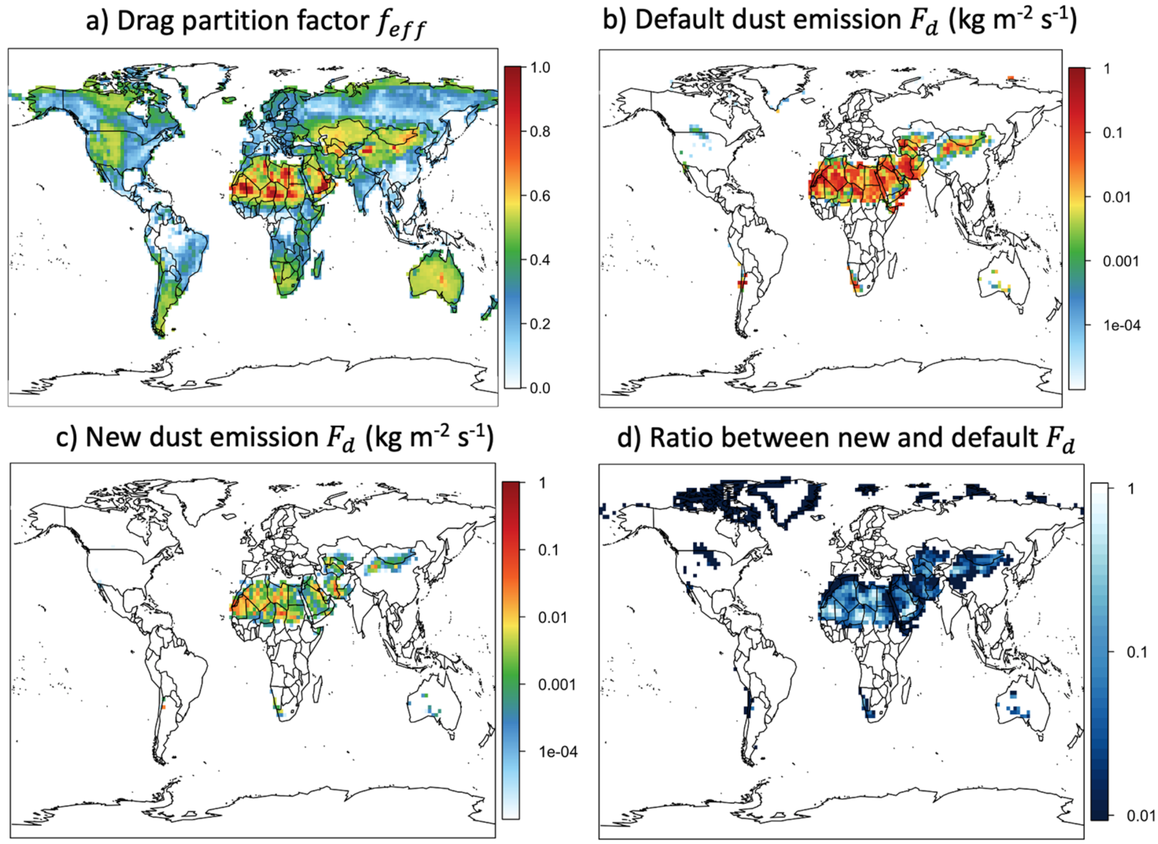

Fig. 8. A CESM sensitivity experiment for year 2012 with and without drag partition effect. (a) The drag partition factor f_{eff} as a coarse version of Fig. 5, as obtained by satellite-derived aeolian roughness length from Prigent et al. (2012) and regridded by the "emission-weighted" average algorithm in Sect. 5. (b) The default CESM dust emissions without the drag partition effect. (c) The dust emissions modified by the drag partition effect. (d) Ratio between dust emissions with drag partition effect and emissions without the effect.

The preliminary simulations increase modeled thresholds especially over regions with large soil grain sizes or with more roughness elements, leading to reduced dust emissions (and thus activation frequencies) into atmosphere.

To further make the spatiotemporal variability of dust thresholds and emissions more realistic, we will incorporate time-varying vegetation roughness in the climate models in the future.

Our future work will include:

- Explore other possible predictors apart from % of total silt to predict D_{p} in the future;
- Implementation of 3-D hybrid drag partition data into CESM with vegetation;
- Instead of inputting diagnostic data, compile CESM codes for prognostic drag partition simulations using CESM LAI;
- We are implementing another drag partition scheme by Okin et al. (2008);
- Compare simulations using different schemes of drag partition;
- Compare our data against AERONET and other AOD observations.

ABSTRACT

A key challenge in accurate simulations of desert dust emission is the parameterization of the threshold wind speed above which dust emission occurs. However, the existing parameterizations yield a unrealistically low dust emission threshold in some climate models such as the Community Earth System Model (CESM), leading to higher simulated dust source activation frequencies than observed and requiring global tuning constants to scale down dust emissions. Here we develop a more realistic parameterization for the dust emission threshold in CESM. In particular, we account for the dissipation of surface wind momentum by surface roughness elements such as vegetation, rocks, and pebbles, which reduce the wind momentum exerted on the bare soil surface. We achieve this by implementing a dynamic wind drag partition model by considering the roughness of the time-varying vegetation as quantified by the leaf area index (LAI), as well as the time-invariant rocks and pebbles using satellite-derived aeolian roughness length. Furthermore, we account for the effect of soil size on dust emission threshold by replacing the currently used globally constant soil median diameter with a spatially varying soil texture map. Results show that with the new parameterization dust emissions decrease by 20–80% over source regions such as Africa, Middle East, and Asia, thereby reducing the need for the global tuning constant. Simulated dust emissions match better in both spatiotemporal variability and emission frequency when compared against satellite observed dust activation frequency data. Our results suggest that including more physical dust emission parameterizations into climate models can lessen bias and improve simulation results, possibly eliminate the use of empirical source functions, and reduce the need for tuning constants. This development could improve assessments of dust impacts on the Earth system.

REFERENCES

Chatenet B. et al.: Assessing the microped size distributions of desert soils erodible by wind, Sedimentology, 43(5), 901–911, 1996.

Hengl T. et al.: SoilGrids250m: Global gridded soil information based on machine learning, PLOS ONE, 12(2), e0169748, 2017.

Kok J. F. et al.: An improved dust emission model – Part 2: Evaluation in the Community Earth System Model, with implications for the use of dust source functions, Atmospheric Chemistry and Physics, 14(23), 13043–13061, 2014.

Marticorena B. et al.: Modeling the atmospheric dust cycle: 2. Simulation of Saharan dust sources, Journal of Geophysical Research: Atmospheres, 102(D4), 4387–4404, 1997.

Menut L. et al.: Impact of surface roughness and soil texture on mineral dust emission fluxes modeling, Journal of Geophysical Research: Atmospheres, 118(12), 6505–6520, 2013.

Okin, G. S.: A new model of wind erosion in the presence of vegetation, Journal of Geophysical Research: Earth Surface, 113(F2), 2008.

Pierre C. et al.: Impact of vegetation and soil moisture seasonal dynamics on dust emissions over the Sahel, J. Geophys. Res., 117, D06114, 2012.

Prigent C. et al.: Comparison of satellite microwave backscattering (ASCAT) and visible/near-infrared reflectances (PARASOL) for the estimation of aeolian aerodynamic roughness length in arid and semi-arid regions, Atmospheric Measurement Techniques, 5(11), 2703–2712, 2012.